ELSEVIER

Ultramicroscopy 71 (1998) 311–319

ultramicroscopy

Near-field optical and shear-force microscopy of single fluorophores and DNA molecules

M.F. Garcia-Parajo*, J.-A. Veerman, A.G.T. Ruiter, N.F. van Hulst

Department of Applied Physics, Applied Optics Group & MESA Research Institute, University of Twente, P.O. Box 217, 7500 AE Enschede, The Netherlands

Abstract

Photodynamics of individual fluorescence molecules has been studied using an aperture-type near-field scanning optical microscope with two channel fluorescence polarisation detection and tuning fork shear-force feedback. The position of maximum fluorescence from individual molecules could be localised with an accuracy of 1 nm. Dynamic processes such as translational and rotational diffusion were observed for molecules adsorbed to a glass surface or embedded in a polymer host. The in-plane molecular dipole orientation could be determined by monitoring the relative contribution of the fluorescence signal in the two perpendicular polarised directions. Rotational dynamics was investigated on 10 ms–1000 s timescale. Shear-force phase feedback was used to obtain topographic imaging of DNA fragments, with a lateral and vertical resolution comparable to scanning force microscopy. A DNA height of 1.4 nm has been measured, an indication of the non-disturbing character of the shear force mechanism.

1. Introduction

The possibility to perform detection of single fluorescence molecules at ambient conditions and/or aqueous solutions, has awakened the interest of researchers from many different disciplines, including analytical chemistry, material research and biological sciences. Great advances have been achieved using ultrasensitive fluorescence detection methods combined with excitation in the optical diffraction-limited regime (far-field) [1–3] or in the near-field regime, using near-field scanning optical microscopy (NSOM) [4–6]. Of particular interest in bioscience, is the possibility of correlating biological functions with movement that is, translational and rotational dynamics.

Observation of translational diffusion at individual molecular level, has been achieved in the far field with a time resolution into the millisecond range, and with the molecules attached to a surface [7], in gels [8] or aqueous solutions [9]. In the near field, the trajectory of individual molecules, embedded in a polymer matrix or adsorbed on glass, could be recorded during more than 1 h before photodissociation with the concomitant lower time resolution [6,10].

* Corresponding author.

0304-3991/98/$19.00
PII S0304-3991(97)00086-7

Rotational diffusion and the exact determination of the molecular dipole orientation, is similarly interesting because it is very sensitive to the molecular size and environment. Fluorescence anisotropy based upon rotational diffusion over ensemble measurements has been a widely used technique in biochemical research being particularly useful on the quantification of protein denaturation and protein-ligand association reactions [11,12]. Recently, it has been used on the study of thermodynamic, kinetic and structural characteristics of single- and double-standard DNA [13]. At present, in the near field polarisation contrast techniques have shown the ability to distinguish between regions of different molecular dipole orientation [4,14,15].

At a single molecular level, rotational dynamics has been monitored using excitation polarisation modulation using far-field techniques [16]. Since in this case, the molecules were widely dispersed over the sample surface, spatial resolution was not a requirement. In this respect, it is widely accepted that for many fundamental studies at single molecular level and where spatial resolution is not important, far-field techniques represent a better choice compared to near field because of its simplicity and lack of tip perturbations [5]. In most real samples, however, it is desirable to address chemical and biological problems at a denser surface coverage and with higher spatial resolution. In specific situations, it is also advantageous to excite the molecules in "snapshots", so that the observation time is prolonged before photo-dissociation occurs. The high spatial resolution, single molecule sensitivity and the ability to correlate optical information with topography information make this technique a powerful approach for the study of many biological systems in their ambient environment. Towards the goal of studying *dynamic processes at the biomolecular level*, we have extended our near-field scanning optical microscope with two polarisation channels and have improved our shear force sensitivity for molecular resolution topographical imaging. In this paper we show that polarisation contrast techniques, combined with near-field optics, allow to probe and follow rotational dynamic processes on a single-molecule basis. Molecular localisation with nanometer accuracy together with shear force imaging of DNA are also presented, illustrating the reliability and long-term stability of our microscope.

2. Experimental set-up and sample preparation

The experimental set-up is schematically shown in Fig. 1. The NSOM was built into a Zeiss Axiovert 135 TV inverted optical microscope [17]. A near-field optical light source consisting of a tapered, aluminium-coated single-mode optical fibre (Newport F-SV) with an aperture of less than 100 nm was used to illuminate the sample. The 514 nm line from an Ar/Kr laser was used as the excitation wavelength and coupled into the coated fibre while the excitation power was adjusted to give about 3 nW at the end of the tip (as measured in the far field). The sample was scanned underneath the fibre and the fluorescence emission for the sample plane was collected with a $100\times$, 1.3 NA oil immersion objective and directed to the detectors. The fluorescence was filtered from the transmitted light using a long-pass filter ($\lambda > 550$ nm). A broad-band polarising beam splitter cube (Newport, 400–700 nm) was used to separate the fluorescence signal into two perpendicular polarisation components and were then directed to the detection channels. Photon counting avalanche photodiodes (APD, SPCM-100 from EG&G Electro Optics) were used as detectors. In the near-field operation the fibre aperture was confocally aligned onto the detectors. Shear-force feedback based on a tuning fork system [18,19] was used to maintain a constant tip–sample separation and to generate high-resolution topographical images.

Background fluorescence from the fibre tip itself was minimised by keeping its length as short as possible (less than 15 cm length) and removing its plastic jacket. The detection efficiency of the optical path was optimised for maximum signal collection (collection efficiency was approximately 10%, including quantum efficiency of the APD detectors). Count rates between 10^3 to 10^4 counts/s per detector from a single molecule were obtained at a background signal of typically 300 counts/s per detector. By imaging a sample area of a few square microns approximately once every 10 min, the

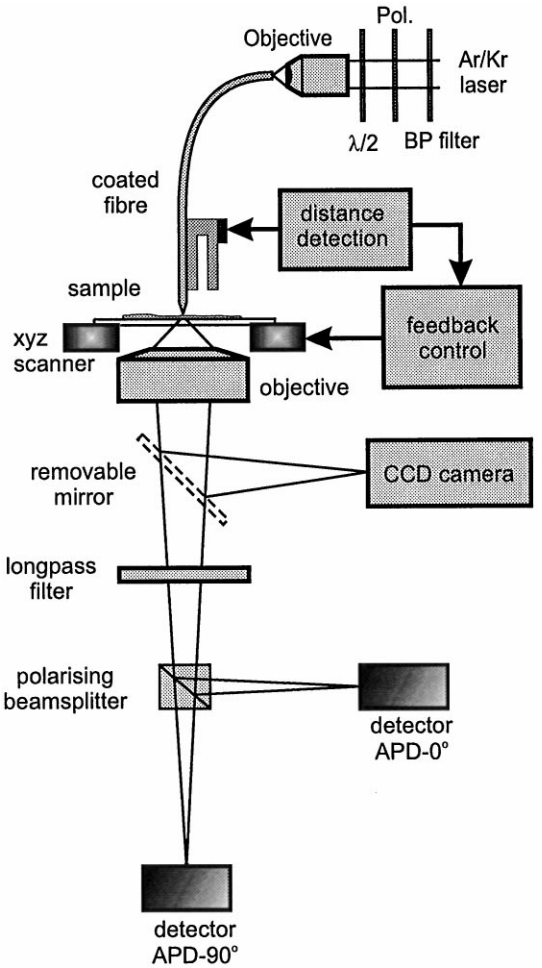

Fig. 1. Schematic set-up of the aperture-type near-field scanning optical microscope (NSOM) with a metal-coated adiabatically tapered fibre. The scanning sample stage is mounted on top of an inverted optical microscope. Shear-force feedback using a tuning fork has been implemented to control the tip–sample distance separation. The fluorescence is collected in transmission using a high NA objective, subsequently split into two perpendicular polarisation directions using a polarising beam splitter and detected with two avalanche photodiodes (APD).

molecules could be traced over more than an hour before photodissociation.

The single molecular fluorescence capability of our NSOM was complemented with improvements on the shear-force detection allowing molecular resolution topographical imaging. The shear force detection was implemented using a quartz piezo-electric tuning fork as a resonant sensor mounted to the fibre probe. The resonance frequency of the combined tuning fork – NSOM tip system was typically 32–34 kHz. The system was driven externally with an oscillation amplitude of approximately 15 pm peak-to-peak, corresponding to a few nanometers lateral displacement of the tip during normal operation, as a result of the system resonance amplification. The phase difference between the excitation signal and the tuning fork signal was detected and used as the feedback signal for the tip–sample distance regulation. In this way, by detecting the phase of the tuning fork response, the bandwidth of the feedback regulation was enhanced to a several hundred Hz [19]. During measurements, the phase set-point was chosen to be close to the out-of-contact value and the scan speed about 1 μm/s, comparable to the integration time needed for single-molecule NSOM imaging. Additionally, three signals related to the shear force control are collected and used to generate three independent images, namely; the z-piezo signal which creates the topographic image, the residual phase signal beyond the feedback bandwidth, and the oscillation amplitude of the tuning fork–tip system.

Samples of rhodamine-6G (R-6G) (Molecular Probes, R-634) were prepared by directly spin coating a 5×10^{-8} M solution of the dye molecules in methanol (Merck, 99.8%) on a clean 170 μm thick glass cover slip. Samples of Carbocyanine (DiI-C_{18}) dye molecules embedded in a thin polymethylmethacrylate (PMMA) layer were prepared in the following way: DiI (Molecular Probes, D-282) molecules were diluted in methanol to a final concentration of 5×10^{-8} M. The dye solution was then added into a 0.5% weight PMMA in chloroform (Merck, 99.4%). A 10–20 μl drop was deposited onto a freshly cleaned 170 μm thick glass cover-slip and spin coated at 4000 rpm. The resulting layer thickness was between 5 and 10 nm with a surface coverage of typically a few dye molecules per square micrometer. DNA samples for shear-force imaging were prepared in the following way: 10 ng/μl of 600–800 bp long double-standard DNA fragments were diluted in 10 mM Hepes, pH 7.4, and 1 mM $ZnCl_2$, giving a final concentration of 1–5 ng/μl for deposition. A 10–20 μl drop was

deposited onto freshly cleaved mica. After letting the sample set for a couple of minutes, it was washed with water (0.5 ml of doubly distilled water from a squirt bottle) and briefly dried in a stream of compressed air before imaging.

3. Results and discussion

3.1. Single molecular fluorescence detection

Fig. 2a–Fig. 2d shows four consecutive images of individual R-6G molecules adsorbed on a glass substrate. The image region is 1.5×1.5 μm (100×100 pixels) and the integration time per pixel, 25 ms. The maximum signal on the molecules was ~ 100 counts/pixel with a background signal of 15 counts/pixel. Individual R–6G molecules are clearly distinguished with a maximum signal-to-background ratio better than 7. From our data, and taking into account molecules that do not show intensity fluctuations nor "blinking", the centre of intensity of the different molecules can be determined with an accuracy of approximately 1 nm [6]. Close inspection of the images reveals relative translational movement of some individual molecules over the glass surface. While some molecules appear to be well located and fixed at the sample surface from frame-to-frame (after compensation for the instrumentation drift), some other molecules show translational trajectories up to 100 nm in a time span of 10 min. As an illustration we show in Fig. 2 molecule 1 which appears to move randomly with respect to molecule 2, which remains fixed on the sample surface. The fact that molecule 1 moves in a random direction and does not show a preferential mobility along the horizontal scan direction suggests that tip-induced effects are not responsible for the observed translational mobility. Besides molecules 1 and 2, other molecules in the image do not seem to be stationary either, although their relative mobility is much lower than molecule 1. In fact, from our experiments we have observed that only a small percentage of molecules adsorbed to glass show some translational mobility.

As mentioned in the introduction, translational diffusion at the molecular level has been observed at different environmental conditions, and a lateral diffusion constant has been estimated in each particular system. The lateral diffusion constant changes orders of magnitude depending on whether the molecules are "free" in solution, with values between 10^{-6} and 10^{-8} $cm^2\ s^{-1}$ [8,9,20], down to values of 10^{-10}–10^{-15} $cm^2\ s^{-1}$ if motion is significantly restricted, as in the case of "immobilised" molecules by attachment to a surface [7,10]. Accordingly, observation times have to correspond to the particular event to follow, i.e., in free-solutions fast temporal detection response on the millisecond scale is needed. In contrast, for molecules embedded in a solid host, time resolution is not a constrain but, observation times ought to be much longer. In our case, with molecules adsorbed to the glass substrate via hydroxyl groups, lateral motion was highly reduced. An estimation of the lateral diffusion constant rendered a value in the order of 10^{-15} $cm^2\ s^{-1}$ [6] which is in agreement with recently reported values for molecules embedded in a polymer host [10]. Additionally, the ability to excite the molecules continuously for approximately 200 ms every 5 s per image, have allowed us to quantify the slow movement of the molecules before photodissociation.

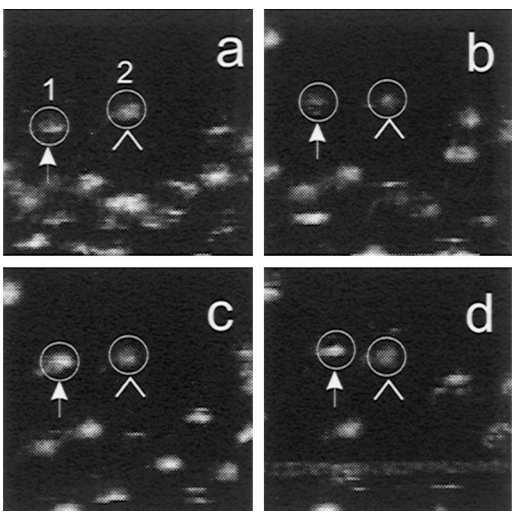

Fig. 2. Translational movement of single R-6G molecules along a glass surface. Four consecutive images of 1.5×1.5 μm^2 have been taken, with a measurement time of 10 min per image. The caret (^) marks a stationary fluorescence molecule, while the arrows track a moving fluorescence molecule.

We have also focused on the observation of single molecular rotational dynamics on a time-scale of 10^{-2}–10^{3} s before photodissociation occurred. As an example, we show in Fig. 3 sequential frame images of DiI molecules embedded in PMMA over the same sample region. The image region was 1.5×1.5 μm (100×100 pixels) with an integration time of 15 ms per pixel. The signal maximum was approximately 100 counts/pixel and the background ~ 5 counts/pixel, leading to a maximum signal-to-background ratio ~ 10. The total time of observation until photobleaching of all molecules was approximately 65 min. We show in Fig. 3 some of the most relevant frames (identified by a number in the between of the images). In each measurement we collect two data sets, one for each fluorescence polarisation direction. Hence, the images on the left column have been obtained by detecting the 0° component of the fluorescence signal (respect to the line-scan direction) and the column on the right has been obtained by detecting the perpendicular contribution of the fluorescence signal. Rotation of the molecular dipole orientation is readily observable for molecules depicted as *a* and *b*. For instance, in frame 1, molecules *a* and *b* are present in both channels. Their particular molecular orientation can be determined by accounting for the relative contributions of the 0° and 90° detection channels: a rough estimation of 40° to 45° in-plane molecular orientation is obtained by calculating the arc tangent of the square root of the ratio of the measured maximum intensities of the molecules in the two detection channels. In frame 2, we presume that molecule *b* has rotated to the 90° direction since no detected contribution in the 0° direction has been observed, while molecule *a* preserves its relative molecular orientation as in frame 1. In frame 3, molecule *b* does not emit light in any of the channels, reappearing in frame 4 with a larger intensity as compared to frame 1. The same molecule is "off" again in frame 5 and finally emits fluorescence once more in frame 6. Similarly, molecule *a* shows preferential rotation to the 90° polarisation detection channel in frames 3 and 4 and present in both channels during frame 5. Persistent non-emission of molecule *a* in subsequent frames suggests that the molecule has photodissociated. Finally, frame 7 shows the

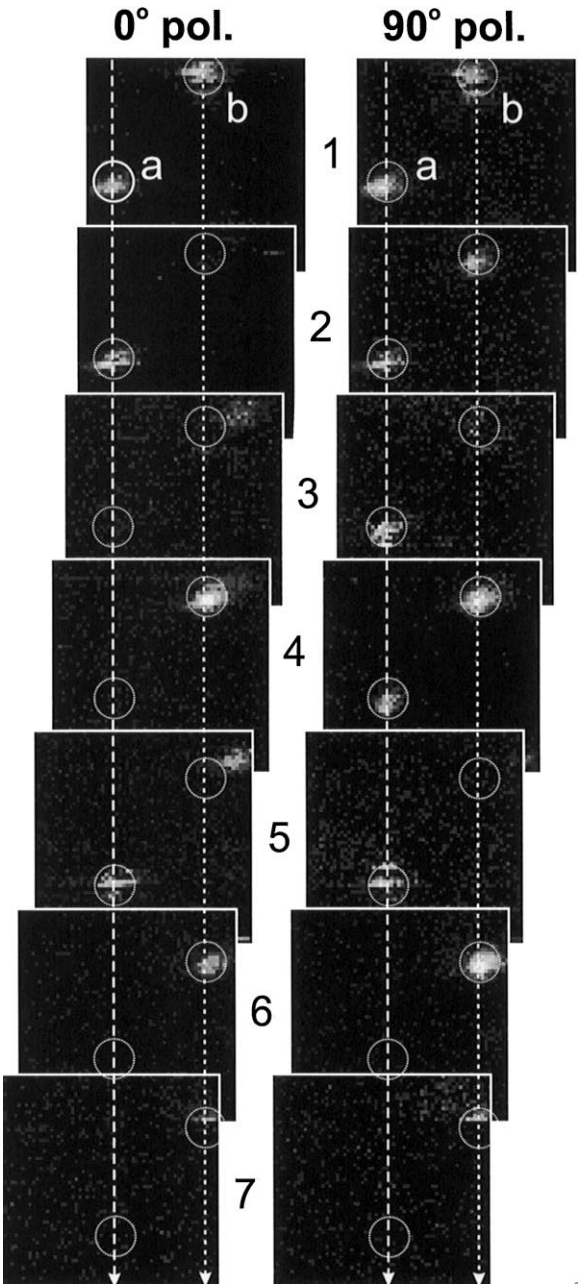

Fig. 3. Rotational activity of single DiI molecules embedded in a PMMA thin layer. Seven frames are selected to illustrate the rotation of the molecular dipole moment of two particular molecules. The frames are vertically arranged to correct for the piezo drift and the vertical arrows serve as a "guide eye" to track the molecules. The two columns display the relative contributions of the fluorescence signal in the two perpendicular polarisation channels (see text for details).

discrete photobleaching of molecule *b* while imaging.

Not all molecules investigated with our NSOM show rotational activity. In fact, most of the molecules, especially the ones embedded in PMMA showed stationary dipoles with relative constant intensities in both detection channels. An example of a typical stable molecule is illustrated in Fig. 4a, where the maximum relative intensity on both channels is plotted for each frame image. Only minor fluctuations on the intensity (within the noise level) are observed. The sudden bleaching of the molecule is observed in frame 8. In contrast, Fig. 4b shows the intensity plot versus frame image of a different molecule that exhibits large intensity fluctuations and transitions between emitting and non-emitting states on a timescale of minutes. The large fluctuations in intensity and the sudden appearance/disappearance of the molecules can be attributed to out of the plane rotations and/or sudden changes in the molecular photophysics. In the first case, rotation of the molecular dipole out of the plane can occur, decreasing the overlap with the excitation and lowering the emission efficiency with maximum intensities obtained with the molecular dipoles lying completely flat on the sample surface, and parallel to the excitation. In the second case, the molecule would retain its orientation, but would undergo spectral fluctuations (probably induced by the local environment) driving the absorption spectrum away from the excitation laser wavelength [5,16,21]. More experiments are currently in progress to distinguish spectral jumps from rotational dynamics. From our results we have observed that both, translational and rotational activity together with possible spectral fluctuations are manifest at peculiarly long timescales, and indication of the influence of the local environment. NSOM affords the possibility to monitor these single molecular processes with high spatial resolution.

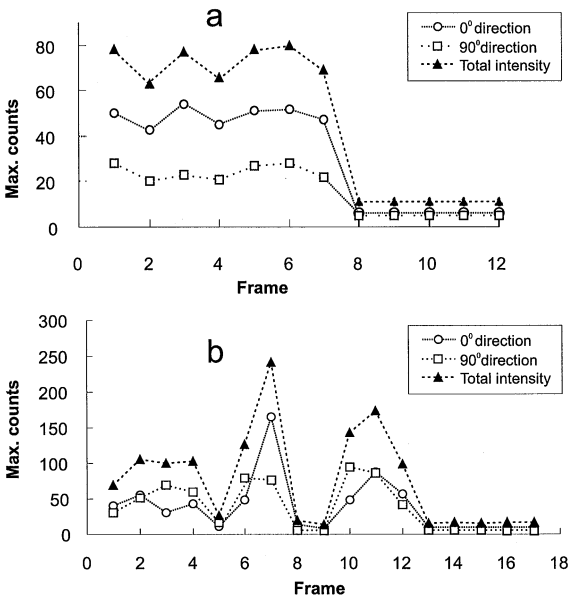

Fig. 4. Maximum intensity versus frame number plotted for two arbitrary DiI molecules. The maximum intensity contributions for each detection channel are plotted as well as the total intensity. The time interval between frames in 5 min. Discrete photobleaching (signature of an individual molecule) is recognised as a persistent cease of emission. A stationary molecule (a), is identified by constant intensity emission in both channels, while large intensity fluctuations and transitions between emitting and non-emitting states are observed for molecule (b).

3.2. Shear-force imaging of DNA molecules

The possibility to perform single molecular fluorescence detection and ability to follow dynamic processes with high spatial resolution brought us to the aim of studying biomolecular events without invading the process itself. Our first goal has been to complement single molecular optical detection with single molecular topography imaging. Fig. 5 shows shear-force images of double-standard DNA fragments using a freshly pulled optical fibre tip. The images have been generated by using the *z*-piezo (a), residual error phase (b) and the rms-oscillation amplitude (c) signals. The contrast on these images are clearly understood by noticing that Fig. 5a corresponds to the topographic image, while Fig. 5b reflects the residual phase on the feedback control loop (see also line trace on Fig. 5d). The negative contrast obtained in Fig. 5c shows the slight decrease of amplitude while scanning over the DNA fragments at constant phase and suggests a different kind of interaction between tip–mica and tip–DNA. The topographic image (a) shows clearly resolved strands, 200–300 nm in length, with a lateral width of 24 ± 2 nm at half-

height and a height of 1.4 ± 0.2 nm, as inferred from cross-sections at the DNA filaments, depicted in Fig. 5d. While the lateral resolution is slightly worse compared to the case of scanning force microscopy (SFM) measurements, the DNA height is larger than the value of 0.5–0.7nm reported with SFM techniques [22–24] and much closer to the 2 nm expected for B–DNA in solution. The reduced DNA height in SFM imaging has been commonly attributed to indentation of the DNA [25], adhesion effects by the contacting tip [26] and the dehydration of the DNA in the air-dried samples [27]. In our case, we believe that only dehydration may have played a role on the reduced measured height since the tip makes no physical contact with the sample. Furthermore, we did not notice any degradation nor incisions on the DNA strands even after repetitive scanning of the same area. These results suggest that shear force imaging is an interesting alternative technique for high-resolution imaging of soft material and, in particular, for the study of DNA-protein interactions that require "loose" immobilisation of the DNA onto the flat surface. The lateral resolution will mainly depend on the residual lateral oscillation amplitude and the tip radius of the fibre probe, which can, in principle, be made down to a few nanometers [28].

We have also performed imaging of DNA using a standard metal-coated NSOM tip. While the lateral resolution decreased slightly as a result of the grainy structure of the tip-end region, the vertical sensitivity remained the same. The measured DNA height was similar to the value obtained with an uncoated tip, i.e., 1.4 ± 0.2 nm. These results are in contrast with recently reported values using the shear-force mechanism to image DNA and where a height of only 0.6 nm has been measured [29]. Real physical indentation of the tip to the DNA or adhesion artifacts may have played a role on the exact determination of the sample height, aside from dehydration effects.

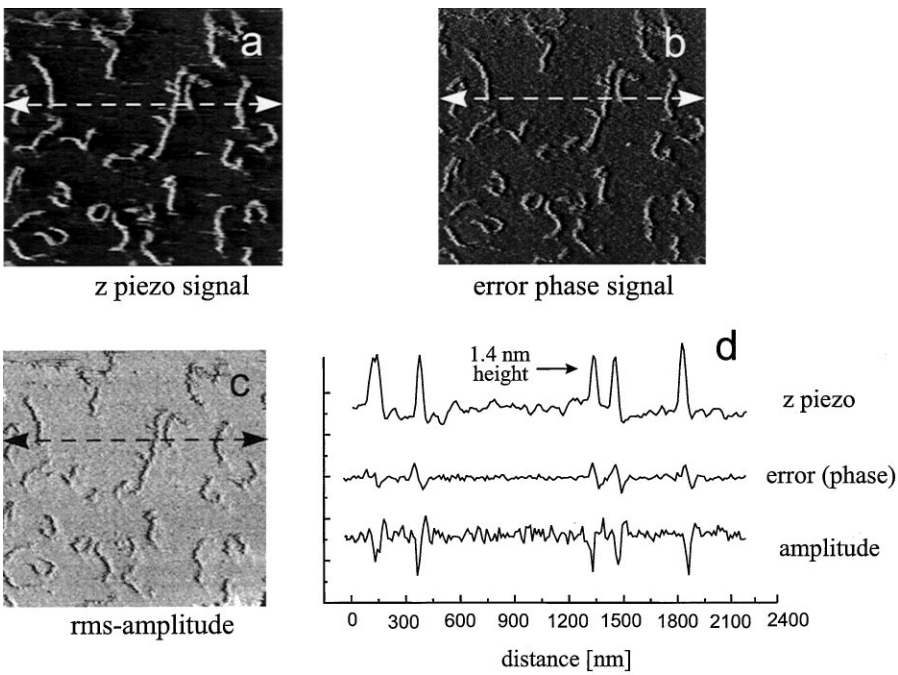

Fig. 5. $2.2 \times 2.2\ \mu m^2$ shear force image of double stranded DNA fragments as deposited on mica, using an uncoated fibre tip. DNA filaments, 600–800 bp long, with a lateral width of 24 ± 2 nm and a height of 1.4 ± 0.2 nm are observed. The images have been generated using (a) the z-piezo signal, (b) the residual phase signal used for feedback control, (c) the rms-oscillation amplitude of the tuning fork. (d) shows three lines traces at the marked positions depicted in (a)–(c).

4. Conclusions

Single-molecule fluorescence detection sensitivity has been demonstrated using a near-field optical microscope extended with a polarisation discriminating detection scheme. Fluorescence from individual molecules could be localised with a resolution of approximately 1 nm, due to the sub-diffraction limited resolution of NSOM. Slow dynamic processes such as translational and rotational diffusion were observed on molecules adsorbed to a glass surface or embedded in a PMMA layer. The in-plane molecular dipole orientation could be determined by monitoring the relative contribution of the fluorescence signal in two perpendicular polarised directions. Rotational dynamics was investigated on 10 ms–1000 s timescale. Shear force phase feedback was used to obtain topographic imaging of DNA fragments, with a lateral and vertical resolution comparable to SFM techniques. Because the shear force mechanism does not requires physical contact with the specimen, degradation of the sample is minimised, making of the technique an alternative tool for the investigation of molecular events without invasion or disruption of the process itself.

The technique offers several advantages compared to far-field optical microscopy: (a) NSOM imaging exhibits super resolution; (b) by virtue of the near-field source, the excitation volume is smaller, allowing higher molecular density and less bleaching of the surrounding; (c) topographical information from the shear-force feedback allows real space mapping of biological material with nanometric resolution without invasion of the specimen itself; (d) mapping and colocalisation studies can be performed at an individual molecular level due to the exquisite sensitivity of the instrument. Unfortunately, despite the promising advantages near-field can offer, one should bear in mind the compromises that have to be made in exchange: the disturbing character of the technique due to the presence of the tip in close interaction to the specimen. Additionally, heating effects close to the tip end might damage biological samples if the excitation intensity is not limited. This in turn reduces the possibility of observing fast dynamical events.

Acknowledgements

The authors thank: Claire Wyman of Erasmus Universiteit Rotterdam (NL) and John van Noort for DNA preparation and fruitful discussions; Kees var der Werf, Frans Segerink, Wouter Rensen, Ine Segers, Margot Snel, Oscar Willemsen and Bart de Grooth for their assistance and suggestions. Maria Garcia-Parajo is financed by the European HCM network on "Near-field Optics for Nano-scale Science and Technology". Joost-Anne Veerman and Ton Ruiter are supported by the Dutch Foundation for Fundamental Research (FOM).

References

[1] R.A. Keller, W.P. Ambrose, P.M. Goodwin, J.H. Jett, J.C. Martin, M. Wu, Appl. Spectrosc. A 12 (1996) 50.
[2] C. Zander, M. Sauer, K.H. Drexhage, D.-S. Ko, A. Schulz, J. Wolfrum, L. Brand, C. Eggeling, C.A.M. Seidel, Appl. Phys. B 63 (1996) 517.
[3] J.J. Macklin, J.K. Trautman, T.D. Harris, L.E. Brus, Science 272 (1996) 255.
[4] E. Betzig, R.J. Chichester, Science 262 (1993) 1422.
[5] X.S. Xie, Acc. Chem. Res. 29 (1996) 598, and references therein.
[6] A.G.T. Ruiter, J.-A. Veerman, M.F. Garcia-Parajo, N.F. van Hulst, J. Phys. Chem. A 101 (1997) 7318.
[7] R.D. Vale, T. Funatsu, D.W. Pierce, L. Romberg, Y. Harada, T. Yanagida, Nature 380 (1996) 451.
[8] R.M. Dickson, D.J. Norris, Y.-L. Tzeng, W.E. Moerner, Science 274 (1996) 966.
[9] X.-H. Xu, E.S. Yeung, Science 275 (1997) 1106.
[10] M.A. Bopp, A.J. Meixner, G. Tarrach, I. Zschokke-Graenacher, L. Novotny, Chem. Phys. Lett. 263 (1996) 721.
[11] M. Velez, D. Axelrod, Biophys. J. 53 (1988) 575.
[12] J.R. Lakowicz, in: Principles in Fluorescence Spectroscopy, Ch. 5, Plenum Press, New York, 1983.
[13] G. Vamosi, C. Gohlke, R.M. Clegg, Biophys. J. 71 (1996) 972.
[14] M.H.P. Moers, H.F. Gaub, N.F. van Hulst, Langmuir 10 (1994) 2774.
[15] D.A. Higgins, D.A. Vanden Bout, J. Kerimo, P. Barbara, J. Phys. Chem. 100 (1996) 13794.
[16] T. Ha, Th. Enderle, D.S. Chemla, P.R. Selvin, S. Weiss, Phys. Rev. Lett. 77 (1996) 3979.
[17] N.F. van Hulst, M.H.P. Moers, IEEE Eng. Med. Biol. (1996) 51.
[18] K. Karrai, R.D. Grober, Appl. Phys. Lett. 66 (1995) 1842.
[19] A.G.T. Ruiter, J.A. Veerman, K.O. van der Werf, N.F. van Hulst, Appl. Phys. Lett. 71 (1997) 28.

[20] Th. Schmidt, G.J. Schütz, W. Baumgartner, H.J. Gruber, H. Schindler, Proc. Natl. Acad, Sci. USA, Biophysics 93 (1996) 2926.
[21] J. Trautman, J.J. Macklin, Chem. Phys. 205 (1996) 221.
[22] C. Bustamante, J. Vesenka, C.L. Tang, W. Rees, M. Guthold, R. Keller, Biochemistry 31 (1992) 22.
[23] M. Bezanilla, S. Manne, D.F. Laney, Y.L. Lyubchenko, H.G. Hansma, H.G. Langmuir 11 (1995) 665.
[24] A. Schaper, J.P.P. Starink, T.M. Jovin, FEBS Lett. 355 (1994) 91.
[25] C. Wyman, E. Grotkopp, C. Bustamante, H.C.M. Nelson, EMBO J. 14 (1995) 117.
[26] S.J.T. van Noort, K.O. van der Werf, B.G. de Grooth, N.F. van Hulst, N.F.J. Greve, Ultramicroscopy 69 (1997) 117.
[27] L.I. Pietrasanta, A. Schaper, T.M. Jovin, Nucleic Acids Res. 22 (1994) 3288.
[28] M.F. Garcia-Parajo, T. Tate, Y. Chen, Ultramicroscopy 61 (1995) 155.
[29] A.K. Kirsch, C.K. Meyer, T.M. Jovin, J. Microsc. 185 (1997) 396.